www.amlett.com, www.vbripress.com/aml, DOI: 10.5185/amlett.2015.5926 Published online by the VBRI Press in 2015

Preparation and physical characterization of CdTe thin films deposited by vacuum evaporation for photovoltaic applications

Subhash Chander*, M. S. Dhaka

Department of Physics, Mohanlal Sukhadia University, Udaipur 313001, India

*Corresponding author. Tel: (+91) 294-2410009; Fax: (+91) 294-2423641; E-mail: sckhurdra@gmail.com

Received: 31 March 2015, Revised: 01 July 2015 and Accepted: 07 July 2015

ABSTRACT

The present communication reports the preparation and physical characterization of CdTe thin films for photovoltaic application. The thin films of thickness 660 nm and 825 nm were deposited on glass and ITO coated glass substrates employing thermal vacuum evaporation deposition method. These as-deposited films were characterized using XRD, UV-Vis spectrophotometer, source meter, SEM and AFM for physical properties. The XRD patterns reveal that the films are crystallized zinc-blende structure of cubic phase with preferred orientation (111) as well as polycrystalline in nature. The optical and crystallographic parameters are calculated and widely discussed. The optical band gap is found in the range 1.52 - 1.94 eV and observed to decrease with thickness. The current-voltage characteristics show that the current is found to be decreased with thickness and the resistivity is increased. The SEM studies show that the films are homogeneous, uniform and free from crystal defects. The grains in the thin films are similar in size and densely packed. The AFM studies reveal that the surface roughness is observed to increase for higher thickness. The experimental results reveal that the films of thickness 825 nm may be used as absorber layer in CdTe/CdS thin film solar cells due to its optical band gap 1.52 eV which is almost identical with the optimum band gap of CdTe and good crystallinity. Copyright © 2015 VBRI Press.

Keywords: CdTe thin film; vacuum evaporation; characterization; thickness; photovoltaic applications.

Introduction

The development of thin film solar cells is an active area of research and more attention has been paid to the fabrication of low cost, excellent stability, high efficiency thin film solar cells. Nowadays, the compound semiconductor materials have been widely used in various fields like energy, environmental and biomedical. Among these widely used compound semiconductors, cadmium telluride (CdTe) is attracted more attention compared to other materials due to its optimum direct energy band gap 1.45 eV at room temperature, high absorption coefficient (> 105/cm) in the visible range of solar spectrum and high chemical stability. It has zinc blende cubic structure with a lattice constant of 6.481Å. [**1-4**]. Therefore, good quality CdTe thin films are presumed to be an ideal optical material and widely used in various electronic and large area optoelectronic devices like solar cells, γ-ray detectors, infrared windows, photo detectors, LEDs, lasers etc. [**5-7**]. At present, this material is receiving renewed interest due to the search for cheaper technologies for large area production of solar cells. The theoretical conversion efficiency of polycrystalline CdTe thin film solar cells is high (29%) and maximum reported conversion efficiency is 20.4% [**8, 9**]. The increase in surface area and the quantum confinement effects make nanostructured materials quite different from their bulk form. The preparation methods and deposition conditions are very important for fabrication of CdTe thin film to achieve high conversion efficiency.

The CdTe thin films can be prepared by a number of deposition techniques such as magnetron sputtering, pulsed laser deposition, spray pyrolysis, electrodeposition, close-space sublimation, metal organic chemical vapor deposition, screen printing, thermal vacuum evaporation etc. [**4, 8, 10-14**]. The thermal vacuum evaporation deposition is one of the most commonly used and suitable technique to prepare CdTe thin films because it has advantages like most productive, very high deposition rate, low material consumption and low cost of operation. The roughness of CdTe thin films on glass substrate was carried out by Leal *et al.* [**15**] using hot wall epitaxy technique and found that the growth surface had a self-affine character with roughness. The effects of adding carbon nanotubes to carbon back electrodes in polycrystalline CdTe thin-film solar cells was investigated by Okamoto *et al.* [**16**] who observed that the improvement in fill factor was mainly due to decrease in series resistance of CdTe solar cells. They also observed that the open circuit voltage was improved after carbon nanotube addition. The role of substrate surface alteration in fabrication of CdTe nanowires was analyzed by Neretina *et al.* [**17**] who concluded that the size uniformity and lateral growth were improved with substrate surface alteration. The effect of annealing time of $CdCl_2$ vapor treatment on CdTe/CdS interface properties was

carried out by Riech *et al.* [**18**]. They found that the intensity of photoluminescence peak of CdTe and CdS regions were drastically changed with chlorine activation and leads to red-shift of the emission spectra. Recently, the effect of post-deposition thermal annealing on the physical properties of vacuum evaporated CdTe thin films was reported by Chander and Dhaka [**19**] who found that the optical band gap and electrical conductivity were decreased with annealing temperature. The influence of trap states on the charge transport in mixed CdTe and CdSe colloidal nanocrystals films was carried out by Gayer *et al.* [**20**] and they concluded that the electron trapping state on the surface of CdTe nanocrystals dominate the conduction in all devices. Hence, the physical and chemical properties of the thin films are strongly dependent upon the preparation techniques, film thickness, pressure, annealing treatment, substrate temperature etc. The annealing may be performed in vacuum, air and gaseous medium like nitrogen, hydrogen, argon etc.

The present paper reports the preparation and physical characterization of polycrystalline CdTe thin films for photovoltaic applications employing a low cost thermal vacuum evaporation deposition technique onto the glass and indium tin oxide (ITO) coated glass substrates. The effect of film thickness on the structural, optical, electrical and surface morphological properties have been investigated by X-ray diffraction, UV-Vis spectrophotometer, source meter, scanning electron microscopy coupled with energy dispersive spectroscopy and atomic force microscopy respectively. The variation in crystallographic parameters like lattice constant, inter-planner spacing, grain size, internal strain, dislocation density and number of crystallites per unit area with respect to film thickness has also been evaluated. The importance of these as-deposited CdTe thin films is in solar cells as absorber layer. The paper is organized as: the first section comprises introduction and review of literature. The second section is devoted to the experimental techniques. The results and discussion part is included in the third section and the forth section embraces conclusions.

Experimental

Fabrication of CdTe thin films

The cadmium telluride powder of purity 99.999% was procured from Sigma Aldrich, USA. The films of thickness 660 nm and 825 nm were deposited on 7059 corning glass and ITO coated glass substrates of dimension (10 mm × 10 mm × 1 mm) employing thermal vacuum evaporation technique at ambient temperature. The substrates cleaning plays an important role during the deposition process, therefore, the substrates were cleaned with double distilled water, acetone followed by isopropyl alcohol and kept on the substrate holder. A tantalum boat was used inside the vacuum chamber to keep the pellets of CdTe. The vacuum chamber was evacuated to a working pressure 2×10^{-6} mbar using diffusion pump and rotary pump combination along with liquid nitrogen trap. The pressure in vacuum chamber was measured by Pirani-Penning gauge combination. The distance between source and substrate was about 15 cm. The evaporation rate was controlled using a quartz crystal monitor and kept constant throughout the sample preparation. The thickness of samples was verified by stylus profile-meter (Ambios, XP-200).

Characterizations of the CdTe thin films

Structural analysis: The crystal structure of as-deposited thin films was analyzed employing an XRD (Panalytical X Pert Pro) of CuKα radiation (λ=1.5406Å) in the range 20°-70°. The intensity data were collected using the step scanning mode with small interval 0.02° to get reasonable number of counts.

Optical analysis: The optical measurements were carried out employing a UV-Vis NIR spectrophotometer (Perkin Elmer LAMBDA 750) at room temperature with normal incidence of light in a wavelength range 250-800 nm.

Electrical analysis: The transverse dark current-voltage (I-V) measurements were performed by a programmable high precision source-meter (Agilent B2901A). The contacts for electrical measurements were made using adhesive silver conductive paste (Sigma Aldrich) on ITO coated glass samples. The I-V characteristics were monitored by SMU Quick I-V measurement software.

Surface morphological and compositional analysis*:* The FESEM images of as-deposited CdTe thin films were taken employing scanning electron microscopy (Nova Nano FE-SEM 450) coupled with energy dispersive spectrometer (EDS). The compositional analysis of the film of thickness 660 nm was performed by the same system with a high accelerating voltage 10 kV and pulse rate 1.72 kcps. The AFM images of as-deposited films were taken by an atomic force microscopy (Multimode 8 Bruker).

Results and discussion

Structural analysis

The X-ray diffraction patterns of as-deposited CdTe thin films of thickness 660 nm and 825 nm is shown in **Fig. 1**. The X-ray diffraction pattern of as-deposited CdTe thin films show diffraction peaks at positions 2θ = 24.25°, 40.22° and 45.26° for film thickness 660 nm which are well indexed corresponding to prominent orientation (111) and two other weak orientations (220) and (311) respectively of JCPDS X-ray powder file data 75-2086 and 15-0770 [**21**]. The angular position of the prominent orientation (111) slightly shifts toward lower (2θ = 23.77°) for film of thickness 825 nm which may be attributed to increase in lattice constant and these as-deposited films crystallize in cubic phase with preferred orientation (111). The intensity of preferred orientation (111) is observed to be slightly increased for thickness 825 nm due to the growth of the materials incorporated in the diffraction process which revealed the good crystallinity [**22**]. The films are highly ordered with a strong reflection along the (111) orientation of the cubic phase and the intensities of the (220) and (311) orientations are extremely low in comparison to the (111) orientation which revealed zinc blende cubic structure of the films with polycrystalline nature. The results are good for the use of these films in CdS/CdTe heterojunction solar cells as absorber layer. The results are in good agreement with the earlier reported works of Ding *et al.* and Paudel *et al.* [**8, 23**]. The crystallographic parameters like lattice constant (a), inter-planar spacing (d), crystallite size (D), internal strain

(ε), dislocation density (δ) and number of crystallites per unit area (N) were calculated and tabulated in **Table 1**.

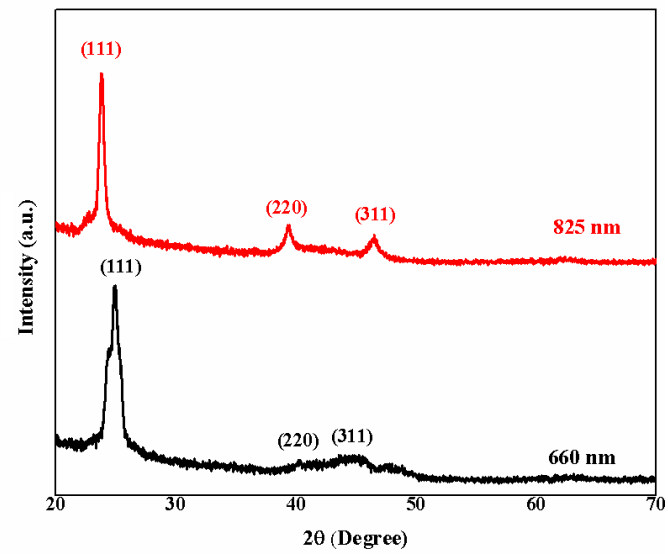

Fig. 1. The X-ray diffraction patterns of CdTe thin films of thickness 660 nm and 825 nm.

Table 1. The crystallographic parameters of CdTe thin films of different thickness.

Thickness	2θ (°)	(hkl)	d (Å)		a (Å)		D (nm)	ε×10^{-3}	δ×10^{15}m^{-2}	N×10^{13}m^{-2}
			Obs.	Std.	Obs.	Std.				
660 nm	24.25	(111)	3.667	3.691	6.449	6.481	14.08	12.23	5.03	2.36
	40.22	(220)	2.239	2.242	6.345	-				
	45.26	(311)	2.001	2.024	6.714	-				
825 nm	23.77	(111)	3.740	3.762	6.370	-	6.11	28.75	26.75	36.11
	39.35	(220)	2.287	2.183	6.189	-				
	46.51	(311)	1.951	1.998	6.641	-				

The grain size (D) was calculated using Debye-Scherrer formula from the full width at half maxima (FWHM).

$$D = \frac{k\lambda}{\beta_{2\theta}\,Cos\theta} \quad (1)$$

Here, λ is the wavelength of source radiation, k is the Scherrer constant having a value 0.94, $\beta_{2\theta}$ is the FWHM and θ is the Bragg's angle.

The average grain size is varied in the range 6.11-14.08 nm and found to be decreased for higher thickness which may be attributed to the formation of new smaller grains on the surface of larger grains and decrease in FWHM corresponding to orientation (111) which revealed fineness of the grains [**24**]. The lattice constant (a) for cubic phase and inter-planar spacing (d) were evaluated using relation concerned (eq. 2) and Bragg's diffraction formula.

$$a = d\sqrt{h^2 + k^2 + l^2} \quad (2)$$

Here h, k, l are Miller indices.

The lattice constant of CdTe thin films is calculated corresponding to prominent orientation (111) and found 6.441Å and 6.370Å for the films of thickness 660 nm and 825 nm respectively. The CdTe film of higher thickness shows a small lattice constant with respect to the standard lattice constant referred to the powder (6.481Å) [**25**].

It is observed that the lattice constant is found to be decreased slightly for higher thickness owing to an increment in angular position of the (111) orientation. The inter-planar spacing (d) is in good agreement with the standard JCPDS data and found to be increased for higher thickness. The dislocation density (δ) is defined as the length of dislocation lines per unit volume of the crystal and was calculated using Williamson-Smallman relation [**26**].

$$\delta = \frac{1}{D^2} \quad (3)$$

The internal strain (ε) was calculated using the relation concerned [**24**].

$$\varepsilon = \frac{\beta_{2\theta}}{4\tan\theta} \quad (4)$$

The dislocation density and internal strain are varied in the range (5.03-26.75) × 10^{15} m^{-2} and (12.23-28.75) × 10^{-3}, respectively. Both parameters are found to be increased for higher film thickness due to the formation of good crystallinity films. The results are in good agreement with reported work of Salavei *et al.* and Lalitha *et al.* [**12, 24**]. The number of crystallites per unit area (N) was calculated using relation concerned [**27**].

$$N = \frac{t}{D^3} \quad (5)$$

Here, t is the thickness of as-deposited thin films.

The number of crystallites per unit area (N) is found in the range (2.36-36.11)×10^{15}m^{-2} corresponding to prominent (111) orientation and observed to be increased with film thickness due to decrease in average grain size which may be attributed to the growth of smaller grains on the surface of larger grains in deposition process.

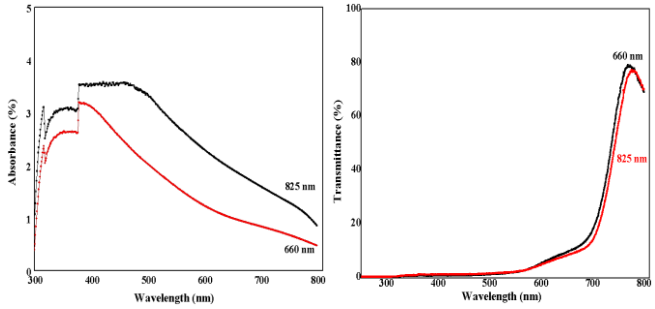

Fig. 2. (a) The absorbance and (b) transmittance spectra of CdTe thin films of thickness 660 nm and 825 nm.

Optical analysis

The optical absorbance and transmittance spectra of as-deposited CdTe thin films are studied in the wavelength range 250-800 nm and presented **Fig. 2**. It is seen from absorbance spectra (**Fig. 2a**) that the absorbance is decreased with wavelength and found more than 3.2% for film of thickness 660 nm. It is found to be higher for the film 825 nm in the visible range which may be attributed to its ordered structure as well as free carrier absorption and revealed the

semiconducting nature of CdTe thin films [**28**]. It is concluded that the more photons in the visible range could be absorbed by CdTe films of thickness 825 nm. As shown in **Fig. 2b**, the optical transmittance spectra of as-deposited films of both thicknesses are consistent with the reported transmittance spectra of CdTe films. The absorption edge of CdTe thin film is mainly distributed between 600 nm and 750 nm and there is a shift of the absorption edge to the longer wavelength with increasing film thickness and red-shift observed which may be attributed to the larger grain size and thermal defects [**8**].

The variation in optical density with wavelength is analyzed to find out the nature of transition and optical energy band gap using the Tauc relation **[5]**.

$$\alpha h\nu = A_0\left(h\nu - E_g\right)^n \quad (6)$$

Here, α is the optical absorption coefficient, h is the plank constant, ν is the frequency of light, A_0 is the characteristics constant as well as a function of density of states near the conduction and valence band edges, E_g is the optical energy band gap, n is the integer and has value n = ½ and 2 for allowed direct and indirect transition respectively. The absorption coefficient and Tauc plot $(\alpha h\nu)^2$ v/s hν of as-deposited CdTe thin films are presented in **Fig. 3.**

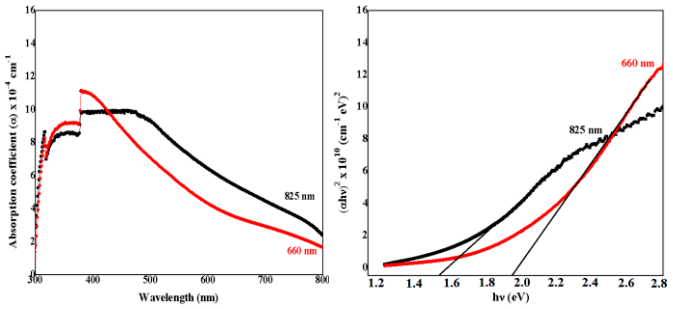

Fig. 3. Absorption coefficient (α) and the Tauc plot (αhν)2 v/s hν of CdTe thin films of thickness 660 nm and 825 nm.

The absorption coefficient (α) was calculated using the following relation.

$$\alpha = \frac{2.303\ A}{t} \quad (7)$$

Here, A is the absorbance and t is the film thickness.

It is observed from Fig.3a that the optical band edge shifts towards the higher wavelength with film thickness. The optical band gap energies were evaluated by extrapolating the straight line of the Tauc plot for zero absorption coefficients (α = 0). Approximately linear nature of the plot is observed towards the lower wavelength and exponentially behavior towards the higher wavelength which indicated the presence of direct optical transition. The exponential behavior of the plot may be attributed to the local impurities or disorder of the materials. The optical energy band gap is found to varied from 1.52 eV to 1.94 eV and observed to be decreased with thickness due to decrease in grain size which may be attributed to the formation of new smaller grains on the surface of larger grains leads to enhance the crystallinity as confirmed by the XRD patterns. The band gap of films of thickness 825 nm are 1.52 eV which is almost identical with the optimum band gap of CdTe films therefore these films may be used as absorber layer in CdTe/CdS thin film solar cells. The calculated optical energy band gap is in good agreement with reported work of Ding *et al.* and Nikale *et al.* [**8, 29**].

The extinction coefficient (k) was calculated using theory of reflectivity of light by relation concerned [**30**] and presented as a function of photon energy in **Fig. 4**.

$$K = \frac{\alpha\lambda}{4\pi} \quad (8)$$

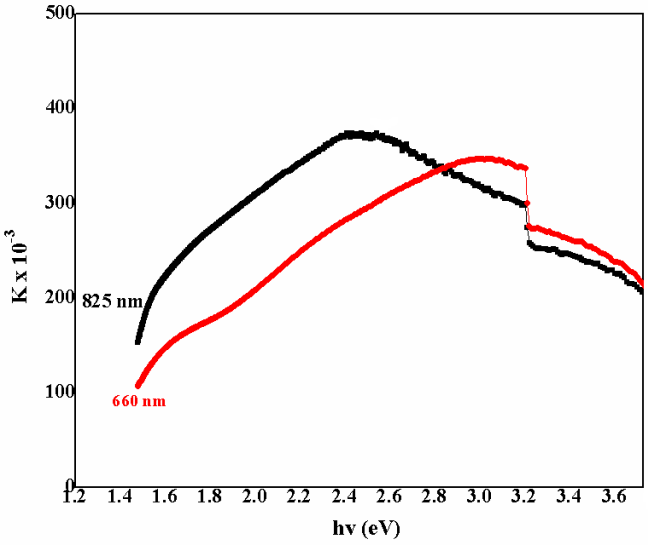

Fig. 4. Variation of extinction coefficient (k) with incident photon energy (hν) in CdTe thin films for different thickness.

The extinction coefficient is increased with photon energy and found maximum at photon energy of 2.4 eV and 3.2 eV for the films of thickness 825 nm and 660 nm respectively, thereafter it is found to be decreased continuously. The extinction coefficient is found to be increased for higher film thickness which may be attributed to the dominance of density effect in the deposited films [**31**].

Electrical analysis

The transverse dark current-voltage (*I-V*) measurements were performed using a programmable high precision source-meter and presented in **Fig. 5**. The variation in current with voltage for both as-deposited CdTe thin films was found to be linear and the current is observed to be decreased with film thickness which may be attributed to the decrement in grain size and grain boundary. Singh *et al.* [**32**] reported a similar behavior for thermally evaporated nanostructured CdTe thin films with substrate temperature. The material quality, electrical and optical properties of the films is strongly depended on the film thickness. The resistivity is found to be increased for higher thickness film 825 nm due to the inverse relation with carrier concentration. The electrical conductivity is found to be decreased for higher thickness which also confirmed the decrease in grain size and grain boundary domains. The results are in good agreement with the earlier reported of Toma *el al.* [**13**] and Al-Ghamdi *et al.* [**33**].

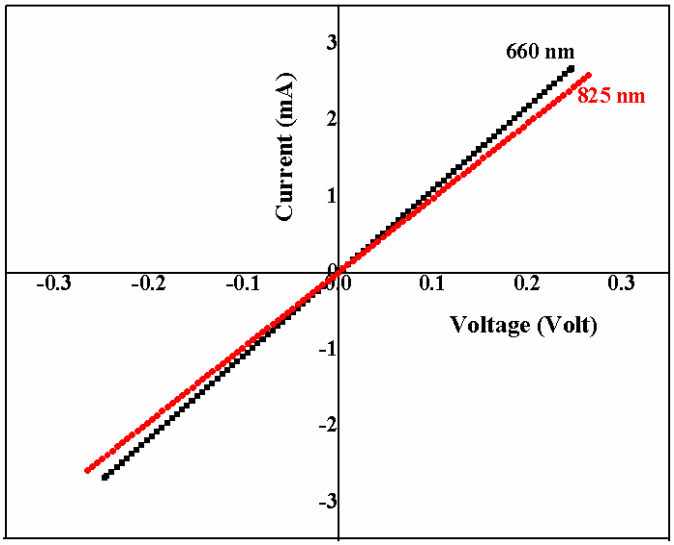

Fig. 5. The transverse current-voltage characteristics of CdTe thin films of thickness 660 nm and 825 nm.

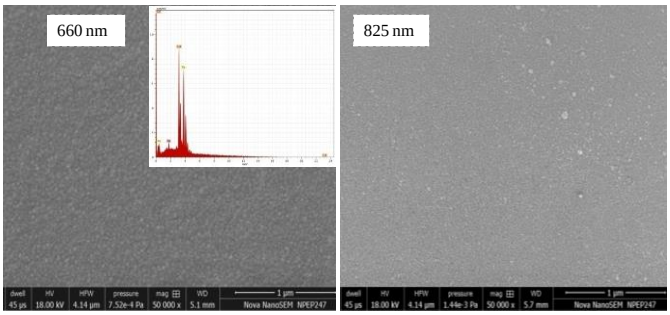

Fig. 6. The image of FESEM of CdTe thin films of thickness 660 nm and 825 nm.

Surface morphological and compositional analysis

The images of field emission scanning electron micrograph (FESEM) of as-deposited CdTe thin films of thickness 660 nm and 825 nm are shown in **Fig. 6**.

The FESEM images of as-deposited CdTe thin films show that the films are homogeneous, fully covered and free from crystal defects like pin holes and cracks. No voids and inclusions have been observed in thin films. The grains in the as-deposited films are similar in size, densely packed and well defined. The small grains and pin holes were observed for the films of thickness 825 nm which could be eliminated by increasing film thickness. The energy dispersive spectrogram (EDS) of as-deposited CdTe film of thickness 660 nm is also indexed in **Fig. 6(a)** which revealed to the presence of Cd and Te element in the as-deposited films. The average atomic percentage of these elements is found to be 52.14% and 44.18% respectively. The results are well supported by earlier reported work [**13, 34**]. The atomic field micrograph (AFM) of as-deposited CdTe thin films of thickness 660 nm and 825 nm are presented in **Fig. 7**.

The AFM images clearly show the polycrystalline nature of the films and how the granular structure changes with the film thickness. The atomic force microscopy was used to determine the surface roughness of the CdTe thin films. The morphology studied show that the grains are compact and similar to each-other. The root mean square roughness is found to be 94.9 nm and 157.3 nm for the film of thickness 660 nm and 825 nm respectively. It is observed to be increased with film thickness which may be attributed to the and increase in porosity due to the three dimensional growth in the films [**35**]. Such increase in roughness with film thickness was also reported by Salavei *et al.* and Reddy *et al.* [**12, 36**] for as-deposited CdTe thin films and ZnO thin films respectively. The increase of root mean square roughness of CdTe films with thickness leads significant effect on the technological applications such as thin film solar cells.

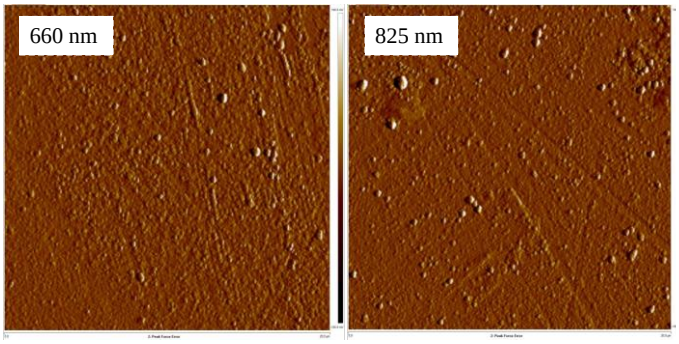

Fig. 7. The AFM image of as-deposited CdTe thin films of thickness 660 nm and 825 nm.

Conclusion

In this study, the preparation and physical characterization of CdTe thin films for photovoltaic applications is reported. The thin films of thickness 660 nm and 825 nm were deposited on glass and ITO coated glass substrates employing thermal vacuum evaporation technique. The X-ray diffraction patterns reveal that the films have zinc-blende structure of cubic phase with preferred orientation (111) and polycrystalline in nature. The optical and crystallographic parameters are calculated and discussed in detail. The average grain size was varied in the range 6.11-14.08 nm and found to be decreased for higher film thickness 825 nm which might be attributed to the formation of new smaller grains on the surface of larger grains. The UV-Vis spectrometer studies show that the optical energy band gap is found in the range 1.52-1.94eV and observed to decrease with thickness. The current-voltage characteristics show that the current is decreased with thickness and the resistivity is observed to increase. The SEM studies show that the as-deposited films are homogeneous, uniform and free from crystal defects. The AFM studies reveal that the surface roughness is observed to be increased for higher thickness films. The experimental results reveal that the films of thickness 825 nm may be used as absorber layer in CdTe/CdS thin film solar cells due to its optical band gap 1.52eV which is almost identical with the optimum band gap of CdTe and good crystallinity.

Acknowledgements

The authors are highly thankful to the University Grants Commission, New Delhi for providing financial support under Major Research Project vide F.No.42-828/2013 (SR) and to the Centre for Non-Conventional Energy Resources, University of Rajasthan, Jaipur for providing deposition facility.

Reference

1. Ismail, B.B.; Gold, R.D. *Phys. Status Solidi A*, **1989**, *115*, 237. **DOI:** 10.1002/pssa.2211150126
2. Chander, S.; Dhaka, M.S. *Mater. Sci. Semicond. Proc.* **2015,** *40*, 708. **DOI:** 10.1016/j.mssp.2015.07.063

3. Chopra, K.L.; Paulson, P.D.; Dutta, V. *Prog. Photovolt: Res. Appl. Appl.* **2004**, *12*, 69. **DOI:** 10.1002/pip.541
4. Mu, Y.; Zhou, X.; Yao, H.; Su, S.; Liv, P.; Chen, Y.; Wang, J.; Fu, W.; Song, W.; Yang, H. *J. Alloys Comp.* **2015,** *629*, 305. **DOI:** 10.1016/j.jallcom.2014.12.203
5. Khairnar,UP.; Bhavsar, DS.; Vaidya, RU.; Bhavsar, GP. *Mater. Chem. Phys.* **2003**, *80*, 421. **DOI:** 10.1016/S0254-0584(02)00336-X
6. Gunjal, S.D.; Khollam, Y.B.; Jadkar, S.R.; Shripathi, T.; Sathe, V.G.; Shelke, P.N.; Takwale M.G.; Mohite, K.C. *Sol. Energy* **2014**, *106*, 56. **DOI:** 10.1016/j.tsf.2004.11.031
7. Pandey, S.K.; Tiwari, U.; Raman, R.; Prakash, C.; Karishna, V.; Dutta, V.; Zimik, K. *Thin Solid Films*, **2005**, *473*, 54. **DOI:** 10.1016/j.tsf.2004.06.157
8. Ding, C.; Ming, Z.; Li, B.; Feng, L.; Wu, J. *Mater. Sci. Engi. B*, **2013**, *178*, 801. **DOI:** 10.1016/j.mseb.2013.03.018
9. Rugen-Hankey, S.L.; Clayton, A.J.; Barrioz, V.; Kartopu, G.; Irvine, S.J.C.; McGettrick, J.D.; Hammond, D. *Sol. Energy Mater. Sol. Cells* **2015,** *136*, 213. **DOI:** 10.1016/j.solmat.2014.10.044
10. Crossay, A.; Buecheler, S.; Kranz, L.; Perrenoud, J.; Fella, C.M.; Romanyuk, Y.E.; Tiwari, A.N. *Sol. Energy Mater. Sol. Cells*, **2012**, *101*, 283. **DOI:** 10.1016/j.solmat.2012.02.008
11. Liyanage, W.P.R.; Wilson, J.S.; Kinzel, E.C.; Dorant, B.K.; Nath, M. *Sol. Energy Mater. Sol. Cells* **2015**, *133*, 260. **DOI:** 10.1016/j.solmat.2014.11.022
12. Salavei, A.; Rimmaudo, I.; Piccinelli, F.; Romeo, A. *Thin Solid Films* **2013,** *535*, 257. **DOI:** 10.1016/j.tsf.2012.11.121
13. Toma, O.; Ion, L.; Girtan, M.; Antohe, S. *Sol. Energy* **2014**, *108*, 51. **DOI:** 10.1016/j.solener.2014.06.031
14. Ban, I.; Kristl, M.; Danc,V.; Danc A.; Drofenik, M. *Mater. Lett.* **2012,** *67*, 56. **DOI:** 10.1016/j.matlet.2011.09.001
15. Leal, F.F.; Ferreira, S.O.; Menezes-Sobrinho, I.L.; Faria, T.E. *J. Phys.: Condens. Matter* **2005**, *17*, 27. **DOI:** 10.1088/0953-8984/17/1/003
16. Okamoto, T.; Hayashi, R.; Ogawa, Y.; Hosono, A.; Doi, M. *Jpn. J. App. Phys.* **2015**, *54*, 04DR01. **DOI:** 10.7567/JJAP.54.04DR01
17. Neretina, S.; Hughes, R.A.; Devenyi, G.A.; Sochinskii, N.V.; Preston, J.S.; Mascher, P. *Nanotech.* **2008**, *19*, 185601. **DOI:** 10.1088/0957-4484/19/18/185601
18. Riech, I.; Pena, J.L.; Ares, O.; Rios-Flores, A.; Rejon-Moo, V.; Rodrıguez-Fragoso, P.; Mendoza-Alvarez, J.G. *Semicond. Sci. Technol.* **2012**, *27*, 045015. **DOI:** 10.1088/0268-1242/27/4/045015
19. Chander, S.; Dhaka, M.S. *Physica E* **2015**, *73*, 35. **DOI:** 10.1016/j.physe.2015.05.008
20. Geyer, S.; Porter, V.J.; Halpert, J.E.; Mentze, T.S.; Kastner, M.A.; Bawendi, M.G. *Phy. Rev. B* **2010**, *82*, 155201. **DOI:** 10.1103/PhysRevB.82.155201
21. Powder Diffraction Data File, Joint Committee of Powder Diffraction Standard, International Center for Diffraction Data, USA Card No. 75-2086 and 15-0770.
22. El-Kadry, N.; Ashour, A.; Mahmoud, S.A. *Thin Solid Films* **1995**, *269*, 112. **DOI:** 10.1016/0040-6090(95)06869-4
23. Paudel, N.R.; Yan, Y. *Thin Solid Films*, **2013**, *549*, 30. **DOI:** 10.1016/j.tsf.2013.07.020
24. Lalitha, S.; Sathyamoorthy, R.; Senthilarasu, S.; Subbarayan, A.; Natarajan, K. *Sol. Energy Mater. Sol. Cells* **2004,** *82*, 187. **DOI:** 10.1016/j.solmat.2004.01.017.
25. Moutinho, H.R.; Al-Jassim, M.M.; Abufoltuh, F.A.; Levi, D.H.; Dippo, P.C.; Dhere, R.G.; Kazmerski, L.L. *26th IEEE Photovoltaic Specialists Conference, Anaheinm, CA,* September 29-October 3, **1997**, *3*. **DOI:** nrel.gov/docs/legosti/fy97/22944.pdf
26. Purohit, A.; Chander, S.; Nehra, S.P.; Dhaka, M.S. *Physica E* **2015,** *69*, 342. **DOI:** 10.1016/j.physe.2015.01.028
27. Dhanam, M.; Prabhu, R.R.; Manoj, P.K. *Mater. Chem. Phys.* **2008,** *107*, 289. **DOI:** 10.1016/j.matchemphys.2007.07.011
28. Lalitha, S.; Karazhanov, S.Zh.; Ravindran, P.; Senthilarasu, S.; Sathyamoorthy, R.; Janabergenov, J. *Physica B* **2007,** *387*, 227. **DOI:** 10.1016/j.physb.2006.04.008
29. Nikale, V.M.; Shinde, S.S.; Bhosale, C.H.; Rajpure, K.Y. *J. Semicond.* **2011**, *32*, 033001. **DOI:** 10.1088/1674-4926/32/3/033001
30. Khan, SA.; Al-Hazmi, FS.; Al-Heniti, S.; Faidah, AS.; Al-Ghamdi, AA. *Curr. App. Phys.* **2010**, *10*, 145. **DOI:** 10.1016/j.cap.2009.05.010
31. Al-Ghamdi, A.A.; Khan, S.A.; Nagat, A.; El-Sadek, M.S.A. *Opt. Laser Tech.* **2010**, *42*, 1181. **DOI:** 10.1016/j.*optlastec*.2010.03.007
32. Singh, S.; Kumar, R.; Sood, K.N. *Thin Solid Films*, **2010**, *519*, 1078. **DOI:** 10.1016/j.tsf.2010.08.047
33. Al-Ghamdi, A.A.; El-Sadek, M.S.A.; Nagat, A.; El-Tantawy, F. *Solid Stat. Comm.* **2012**, *42*, 1644. **DOI:** 10.1016/j.ssc.2012.05.029
34. Ikhmayies, S.J.; Ahmad-Bitar, R.N. *Mater. Sci. Semi. Process.* **2013,** *16*, 118. **DOI:** 10.1016/j.mssp.2012.06.003
35. Kakati, N.; Jee, S.H.; Kim, S.H.; Oh; J.Y.; Yoon, Y.S. *Thin Solid Films*, **2010**, *519*, 494. **DOI:** 10.1016/j.tsf.2010.08.005
36. Reddy, R.S.; Sreedhar, A.; Reddy, A.S.; Uthanna, S. *Adv. Mat. Lett.* **2012**, *3*, 239. **DOI:** 10.5185/amlett.2012.3329